AAEC/E124

AUSTRALIAN ATOMIC ENERGY COMMISSION

RESEARCH ESTABLISHMENT

LUCAS HEIGHTS

THE IRRADIATION BEHAVIOUR OF COLD–PRESSED AND SINTERED BERYLLIUM OXIDE DISPERSION FUELS

by

G. L. HANNA

R. J. HILDITCH

Issued Sydney, June 1964

AUSTRALIAN ATOMIC ENERGY COMMISSION

RESEARCH ESTABLISHMENT

LUCAS HEIGHTS

THE IRRADIATION BEHAVIOUR OF COLD-PRESSED AND SINTERED BERYLLIUM OXIDE DISPERSION FUELS

by

G. L. HANNA

R. J. HILDITCH

ABSTRACT

Coarse and fine dispersions of $(U,Th)O_2$ in BeO, prepared by cold-pressing and sintering, were exposed to fission fragment damage by irradiation in a thermalised neutron flux. Irradiation temperatures were between 610 °C and 720 °C and fission densities of 3×10^{19} to 2×10^{20} fissions per cm^3 of compact were achieved.

The dimensional stability of all specimens was very good and the greatest volume expansion was one per cent. Estimated thermal stresses ranged up to 32,000 p.s.i. but no thermal stress failure occurred. The fine and the most dilute coarse dispersions released only 0.1 per cent. of the fission gases but the remaining coarse dispersions released from 0.6 to 4.9 per cent.

Coarse fuel particles were generally cracked after irradiation and, by microscopy, fission fragment damage to the fuel - BeO interfaces was observed in the high burn-up specimens. Fission gas bubbles developed in coarse fuel particles on post-irradiation annealing at 1250 °C and 1500 °C.

CONTENTS

(continued)

1. INTRODUCTION

Initial irradiation experiments on ceramic fuels at the Research Establishment of the Australian Atomic Energy Commission have been directed at evaluating the contribution of fission product damage (by recoil and fragment accommodation) in the dispersion type fuels of urania – thoria solid solutions in beryllium oxide.

Two experiments have now been completed. The first made use of specimens prepared by hot pressing (Hanna, Hickman, and Hilditch 1963 ; and Hanna 1964), and the second used cold–pressed and sintered specimens, as described in this report. Some preliminary results from this experiment have been published (Hanna, Hilditch, and Hickman 1964) but they are reported here in more detail together with the results of further examination.

The rig (X71) was irradiated in HIFAR in a reactor flux which was greater than 99 per cent. thermal. Thus fast neutron damage from the reactor flux was negligible.

2. EXPERIMENTAL

2.1 Specimen Compositions and Preparation

Specimen compositions are given in Table 1. Fuel contents of 5, 15, and 30 volume per cent. $(U,Th)O_2$ were used together with fissile:fertile ratios of 1 : 3, 1 : 1, and 3 : 1 to give a range of fission densities. All specimens contained fuel particles in the 100 – 185 micron range except those numbered 283 and 286 which contained 0 – 20 micron particles.

The preparation of specimens has been described by Reeve (1964) and Reeve and Jones (1964). Coarse fuel particles were prepared by compacting blended UO_2 and ThO_2 powders, crushing the compacts and selecting the required screen fraction, and spheroidising the particles by self abrasion. Dispersion compacts were prepared by mixing the unsintered fuel particles with Brush UOX BeO, hydrostatically pressing the mixture at 20 t.s.i. and sintering for 2 hours at 1625 °C under hydrogen. Fine dispersions were prepared by adding the urania and thoria to the beryllium oxide without prior mixing. They were compacted and sintered under the same conditions as the coarse dispersions.

Compacts were ground to the final dimensions and one specimen of each type was drilled for half its length to provide an ⅛ inch thermocouple pocket.

2.2 Irradiation

The irradiation rig was of the nuclear heated type described by Hanna, Hickman, and Hilditch (1963). Specimens were arranged in two side–by–side stringers (denoted A and B) so that duplicate specimens were in adjacent stringer positions and exposed to similar neutron fluxes. All the drilled specimens were placed in stringer B so that accurate temperature records were obtained for this stringer only; temperatures in stringer A were assumed to be similar to those in stringer B.

Two specimens of each type described in Table 1 were irradiated. The third specimen was used as a heat–treatment control and was given a heat treatment which closely followed that of the equivalent specimen in the B stringer. The fourth specimen was used as an as–fabricated control.

Average time–weighted irradiation temperatures ranged from 610 °C to 730 °C and are given in Table 1. Figure 1 is a temperature history chart for stringer B specimens which shows that considerable temperature variation occurred. The steady rises in temperature were due to the ingress of air to the helium filled rig. Sudden changes in temperature were associated with changes in reactor power and purging of the rig atmosphere with fresh helium (which produced a drop in temperature).

Uranium burn–ups were calculated from the gamma activities of cobalt monitors accompanying each specimen, flux depressions being estimated by the method of Lewis (1955). As a check on these results, chemical determinations of the Cs–137 yields were made for specimens 159 and 265. These results were 20 to 16 per cent. lower than those from the cobalt monitors (see Table 2) and suggest that flux depressions may have been underestimated. However, in view of previous satisfactory results with monitor techniques and the lack of further chemical measurements, the burn–ups derived from monitor activities have been accepted as reasonable values.

2.3 Pre-Irradiation Examination

Before irradiation, specimen dimensions were measured to an accuracy of 0.00025 cm and hydrostatic densities were measured after thorough impregnation using n-octanol as the liquid.

The microstructure of unirradiated specimens was as follows:

(i) The fuel particles of coarse dispersions were well rounded and ranged from spheres to elongated spheroids. They generally appeared to be porous, but close examination revealed that many of the apparent pores were actually inclusions of a size similar to the pores (about $2-5\mu$). Particles frequently had outer shells which were free from pores and inclusions. The grain size of the fuel material was about 10 microns.

(ii) Fuel particles in the fine dispersion were generally about 1 micron across but some particles ranged up to 20 microns.

(iii) X-ray diffraction revealed that the fuel particles in both coarse and fine dispersions were solid solutions. However, solid solution was not uniform, particularly in the fine dispersions.

(iv) The BeO matrixes in the coarse dispersions consisted of elongated, randomly oriented grains measuring up to 100μ long, by 30μ wide. Pores occurred both at grain boundaries and within grains, the latter pores tending to be very fine (about 1 micron). The grain size of the matrix of the fine dispersion was about 5 microns.

(v) Fuel particles appeared to be well 'bonded' to the matrix in all specimens except 273 - 278 where occasional hair-line cavities were observed. The microstructures of these specimens also showed broad "rivers" running between fuel particles; some of these appeared to be cracks but others contained what appeared to be a grey phase which was not identified.

2.4 Post-Irradiation Examination

Before specimens were recovered from their capsules the volume of the gas within the capsules was measured in a gas burette and samples were analysed by mass spectrometry for stable fission-product gas contents.

Specimens were examined macroscopically using a stereo-periscope and photographed at magnifications of 2 - 15 times. Dimensions were measured with a vernier micrometer and displacement densities were determined after impregnation with n-octanol.

The specimens containing thermocouple pockets were slit in half and the drilled portions were sectioned for metallographic examination. Samples were mounted in epoxy-resin, ground on 120 to 600 grit papers and polished for 48 hours on a vibratory polisher. Heat-treated and as-fabricated control specimens were prepared and examined with the irradiated specimens.

The portions of specimens 155, 161, 273, 280, and 284 remaining after metallographic sampling were cut into three discs which were annealed at 1000 °C, 1250 °C, and 1500 °C for one hour and then examined by metallography.

3. RESULTS

3.1 Macroexamination

With the exception of specimens 283 and 284, which were found to be broken in two transversely on recovery from the capsules, specimens showed little macroscopic change after irradiation. The major change was the apparent swelling of fuel particles in coarse dispersion specimens and a network of ridges on specimens 272 and 273 which was similar in appearance to the network of lines observed in the unirradiated microstructures of the specimens. (Compare Figures 2b and 6a).

The fracture in specimen 283 was associated with an angular cavity measuring about 0.15 mm x 0.4 mm which, from its appearance, could have been a fabrication flaw. Specimen 284 fractured in the plane of the bottom of the thermocouple pocket.

3.2 Fission Gas Release

The volumes of stable fission gas isotope released from the specimen are given in Table 3, as well as the releases expressed as percentages of the total isotopic fission yield.

The average isotopic release from specimens 154 and 155 (5^{v}/o coarse $(U,Th)O_2$), and 283 and 284 (15^{v}/o fine $(U,Th)O_2$), was only 0.1 per cent. However, the releases from the remaining coarse dispersion specimens ranged from 0.6 to 4.9 per cent. with no correlation with temperature or fission density.

3.3 Dimension and Volume Changes

Changes in dimensions, volumes, and hydrostatic densities are given in Table 4. The changes in dimensions of all specimens were low, being between 0.1 and 0.37 per cent. In general the diametral and axial expansions were similar. Volume increases calculated from dimension changes agreed very well with those deduced from impregnated density changes but in nearly all cases were slightly lower. There was no correlation of volume change with fission density or temperature, apart from the specimens of highest fission density (272, 273, 283, and 284) which showed the greatest volume and hydrostatic density changes (1.1 to 1.4 per cent.).

The diametral increases and impregnated density changes in specimens 283 and 284 (fine fuel particles) were very similar to those of specimens 272 and 273 which contained coarse fuel particles but had the same composition and fission density. Unfortunately axial expansion could not be compared, owing to the fractures in specimens 283 and 284.

Heat-treated control specimens showed no detectable change in dimensions or hydrostatic densities.

3.4 Microstructure Changes

The typical microstructure of unirradiated and irradiated specimens is shown in Figures 3 - 8.

The following changes were observed in the microstructures after irradiation:

(i) Slight pull-out of grains from the matrixes of coarse dispersions (Figures 3b - 7b). In the more dilute dispersions, it was apparent that pull-out was localised to groups of fuel particles and was absent from regions removed from fuel particles.

(ii) Frequent cracking in coarse fuel particles (for example, Figure 6c) and large irregular voids in the fuel particles of specimens 159, 161, 273, and 280 (Figures 4, 6, and 7). These voids were usually associated with cracks.

(iii) The diffuse nature of the fuel - BeO interfaces in specimens 273 and 283 which both received fission doses of 1.8×10^{20} fissions per cm^3 of specimen or 1.2×10^{21} fissions per cm^3 of $(U,Th)O_2$. (See Figures 8b and 9b).

(iv) Rounded pores appeared in the coarser fuel particles of specimen 283 (fine dispersion) irradiated to 1.2×10^{21} fissions per cm^3 of $(U,Th)O_2$. The pores are illustrated in Figure 8b and are similar in appearance to gas bubbles.

No changes in microstructure were observed after post-irradiation annealing at 1000 °C but the following changes were observed after annealing at 1250 °C and 1500 °C.

(1) Coarse Dispersions

1250 °C: Networks of fine rounded pores had developed in the grain boundaries of fuel particles (Figure 10a). The large irregular voids as seen in the as-irradiated specimens were fewer, though cracks still persisted.

The matrixes of most specimens were unchanged but that of specimen 273 was badly cracked (Figure 10b). Pores had developed at the fuel – BeO interfaces and the interfaces in specimen 273 were sharply defined and had lost the diffuse appearance which they had in the as-irradiated condition.

1500 °C: Considerable coalescence of pores had occurred within fuel grains and the grain boundary networks obvious after the 1250 °C anneal remained only in the dense outer shells of the particles. There were very few cracks and no large irregular pores such as those seen in the fuel of as-irradiated specimens. (Figures 11a and 11b).

Matrixes were micro-cracked in the region of fuel particles but cracking in specimen 273 was less severe than after the 1250 °C anneal (Figure 11b).

Pores had developed at the fuel – BeO interfaces making them very irregular. The diffuse interfaces in specimen 273 had become sharp again and a mottled zone containing fine rounded pores extended for 15 – 20 microns into the matrix from the fuel particle boundaries. (Figure 12).

(2) Fine Dispersions

The only obvious change in fine dispersions was a sharpening of the fuel – BeO interfaces in the samples annealed at 1250 °C and 1500 °C. Other changes which may have occurred were obscured by the fine grain size and by metallographic "pull-out".

4. DISCUSSION

The dimensional stability of all specimens was very good and compared favourably with that of hot-pressed specimens described by Hanna, Hickman, and Hilditch (1963). The dimension and density measurements show that there was negligible change in open porosity and that swelling was due to increases in closed porosity and/or lattice dimensions (see Table 4).

All specimens appear to have had a high resistance to thermal stressing. No specimen showed any sign of thermal stress failure and the only specimens which failed (283 and 284) fractured transversely and not radially as would be expected of thermal stress failure. From the estimated stresses (Table 1) it may be seen that the maximum stress at the surface was over 22000 p.s.i. in several cases and 32000 p.s.i. in one case. The values are thought to be reasonable because, although for calculation the specimens were assumed to be infinitely long rods, the unirradiated value for thermal conductivity was used and some reduction in conductivity would have occurred during irradiation. It appears therefore, that some mechanism of stress relaxation must have operated.

The most perplexing feature of the results was the high fission gas releases from the coarse dispersions containing 15 and 30 volume per cent. of fuel. In these specimens, the releases were much greater than the expected releases by recoil. The only obvious factors that might have contributed to this were the cracking and porosity in fuel particles. These are of doubtful importance however, as (a) both were observed in the 5 volume per cent. dispersions where fission gas releases were low, and (b) cracking would only significantly increase the gas release if release occurred by diffusion rather than recoil. This is unlikely at the temperatures achieved in this experiment. Johnson and Mills (1963) have also reported, but not explained, gas releases from coarse dispersions which were much higher than those from similar fine dispersions.

The large irregular cavities seen in fuel particles (Figures 4 – 7) do not appear to be a true irradiation effect. Their shapes were not typical of fission gas bubbles and there was no further evidence of bubble formation in the as-irradiated specimens. The voids were frequently associated with cracks and it appears most likely that they developed during metallographic

preparation by spalling in the region of the cracks. Post-irradiation annealing at 1250 °C reduced the number of voids and after annealing at 1500 °C both cracks and voids were no longer seen. It seems likely therefore, that in the as-irradiated condition, the fuel particles were highly stressed and spalled easily; it is possible too that strain led to cracking during metallographic preparation rather than during irradiation.

The diffuse fuel-matrix boundary in specimens irradiated to 12 x 10^{20} fissions per cm^3 of $(U,Th)O_2$ (5 a/o heavy metal burn-up) is undoubtedly due to fission fragment bombardment and may be an enforced solid solution or an extremely fine two-phase or multi-phase structure of BeO, $(U,Th)O_2$, and fission products.

Similar interfacial effects in UO_2-BeO specimens were observed by Johnson and Lofftus (1962) at a temperature estimated to be between 950 °C and 1300 °C. The post-irradiation annealing experiments described in Section 3.4 suggest that the effect will not be observed during irradiation at 1250 °C and above and that precipitation of fission products and gas bubbles will occur in a broader region (10 – 15 microns wide) around the fuel particles.

The development of fission gas bubbles within fuel particles on post-irradiation annealing occurred preferentially at grain boundaries; this is consistent with the behaviour of hot-pressed specimens described by Hanna, Hickman, and Hilditch (1963). However, the bubbles were larger in the sintered specimens annealed at 1500 °C and the coalescence of bubbles and pores tended to obscure the grain boundary networks apparent after the 1250 °C anneal. Particles with dense outer shells tended to retain finer bubbles in a grain boundary network in the denser regions so it appears that the larger bubble size in the sintered specimens is probably due to coalescence of bubbles with fabrication pores.

5. CONCLUSIONS

The experiments have shown that the dimensional stability and structural integrity of cold-pressed and sintered dispersions of $(U,Th)O_2$ in BeO are very good when exposed to fission fragment damage in the absence of fast neutron irradiation. Their resistance to thermal stresses also appears to be very good.

The behaviour of these specimens was similar to that of hot-pressed specimens irradiated under similar conditions except that fission gas retention was poorer in several cases. The reasons for this are not clear but may be associated with cracking or the greater porosity in cold-pressed and sintered fuel particles.

6. ACKNOWLEDGMENTS

The authors are indebted to the following for assistance in this experiment: Irradiation Rig Group for assembly and operation of the rig, Hot Cells Operations Group for all post-irradiation handling, Analytical Chemistry Section for burn-up and fission gas analyses, and Fuel Element Development Section for preparation of specimens.

7. REFERENCES

Hanna, G.L., Hickman, B.S., and Hilditch, R.J. (1963). – AAEC/E 106.

Hanna, G.L. (1964). – AAEC/E 125 report in press.

Hanna, G.L., Hilditch, R.J., and Hickman, B.S. (1964). – Proc. Int. Conf. on Beryllium Oxide. North Holland. In press.

Hickman, B.S. (1962). – AAEC/E 90.

Johnson, D.E., and Lofftus, F.H. (1962). – GA – 3483.

Johnson, D.E., and Mills, R.G. (1963). – GA – 4138.

Lewis, W.B. (1955). – Nucleonics 12 (10): 31.

Reeve, K.D. (1964). – Proc. Int. Conf. on Beryllium Oxide. North Holland. In press.

Reeve, K.D., and Jones, K.A. (1964). – AAEC/E 116.

TABLE 1

SPECIMEN COMPOSITIONS, IRRADIATION TEMPERATURES, AND THERMAL STRESSES

Specimen No.	$(U,Th)O_2$ Content v/o	Molar Ratio $UO_2 : ThO_2$	Particle Size of $(U,Th)O_2$ microns	Irradiation Temperature °C		Estimated Thermal Stress p.s.i.
				Mean	Max	
154–157	5	1 : 3	100 – 200	610	725	3000
158–159	15	1 : 3	100 – 200	670	795	12000
160–163	15	1 : 3	100 – 200	675	780	13000
264–267	15	1 : 1	100 – 200	720	850	26000
272–275	15	3 : 1	100 – 200	725	820	24000
279–282	30	1 : 3	100 – 200	730	875	32000
283–286	15	3 : 1	0 – 20	720	940	24000

Note: Thermal stresses were calculated for the period of maximum temperature operation which occurred shortly after irradiation began. The figures apply to the first two specimens in each group.

TABLE 2

BURN–UPS AND FISSION DENSITIES

Specimen No.	Burn–up, a/o (U + Th)			Fission Density Fissions cm^{-3} From Co Monitor Burn–ups	
	Tabulated Fluxes	Cobalt Monitors	Cs–137 Yield	Whole Specimen	Fuel Material
				x 10^{19}	x 10^{19}
154	3.4	2.7		3.3	65
155	3.5	2.6		3.0	60
158	3.0	2.3		8.1	54
159	3.1	2.5	2.02	8.9	59
160	3.2	2.6		9.1	60
161	3.2	2.6		9.0	60
264	6.8	3.95		14	94
265	6.85	3.9	3.35	14	94
272	7.4	4.9		18	118
273	7.5	5.5		20	135
279	2.4	2.0		14	46
280	2.35	1.9		14	46
283	6.0	4.65		17	110
284	6.5	5.0		18	120

TABLE 3

SUMMARY OF FISSION GAS RELEASES

Specimen No.	Volume of Gas Released cc x 10^{-5}							Total Vol. cc x 10^{-5}	Percentage Release of Fission Gas							Mean Percentage Release
	Krypton			Xenon					Krypton			Xenon				
	83	84	86	131	132	134	136		83	84	86	131	132	134	136	
154	N.D.*	N.D.	N.D.	5.7	9.4	22.9	30.0	68	N.D.	N.D.	N.D.	0.09	0.10	0.14	0.22	0.15
155	N.D.	N.D.	N.D.	6.6	17.1	27.6	35.4	86.7	N.D.	N.D.	N.D.	0.13	0.23	0.21	0.33	0.22
158	6.0	19.9	50.7	51.7	86.6	163.2	222.9	601	0.32	0.58	0.74	0.5	0.57	0.59	1.00	0.61
159	14.3	35.0	79.5	82.7	135.2	256.0	345.0	947.7	0.83	1.10	1.25	0.87	0.96	1.00	1.67	1.1
160	11.9	27.4	62.2	54.6	91.5	169.3	218	634.9	0.56	0.71	0.8	0.47	0.54	0.55	0.86	0.64
161	21.0	53.5	100.3	105.0	173.9	319	441	1214	1.15	1.59	1.49	1.04	1.17	1.18	2.02	1.38
264	157	314	628	665	1058	1940	2587	7349	4.89	5.28	5.28	3.7	4.04	4.08	6.69	4.85
265	77	148	289	304	488	901	1216	2423	2.76	2.86	2.79	1.97	2.15	2.18	3.63	2.62
272	420	815	1572	1738	2782	5142	6734	19203	1.47	1.55	1.49	1.1	1.20	1.22	1.97	1.43
273	254.7	501	967	1067	1691	2965	4139	10685	0.93	0.99	0.95	0.7	0.76	0.73	1.26	0.90
279	64.0	124	240	225	377	699	915.0	2644	2.02	2.11	2.05	1.28	1.46	1.49	2.40	1.83
280	40.0	86	173	173	285	529	695.0	1981	1.45	1.67	1.69	1.13	1.26	1.29	2.09	1.51
283	–	–	–	5.3	6.5	14.3	23.8	49.9	–	–	–	0.03	0.025	0.03	0.06	< 0.1
244	–	–	–	7.3	12.8	27.5	36.6	84.2	–	–	–	0.03	0.035	0.04	0.08	< 0.1

* N.D. – Not Detected.

TABLE 4

DIMENSION AND VOLUME CHANGES OF IRRADIATED SPECIMENS

Specimen	Change in Diameter %	Change in Length %	Change in Volume %	Change in Hydrostatic Density (Impregnated) %
154	0.1	0.15	0.35	0.6
155	0.2	0.2	0.6	0.65
158	0.15	0.15	0.45	0.65
159	0.2	0.25	0.65	0.74
160	0.15	0.15	0.45	0.55
161	0.2	0.2	0.6	0.75
264	0.2	0.2	0.6	0.65
265	0.2	0.3	0.7	0.6
272	0.3	0.3	0.9	1.1
273	0.35	0.3	1.0	1.2
279	0.2	0.2	0.6	0.55
280	0.25	0.25	0.75	0.7
283	0.25	Broken		1.2
284	0.25	Broken		1.4

Note: The dimensions of unirradiated heat-treated specimens remained constant to within 0.05 per cent. during heat treatment.

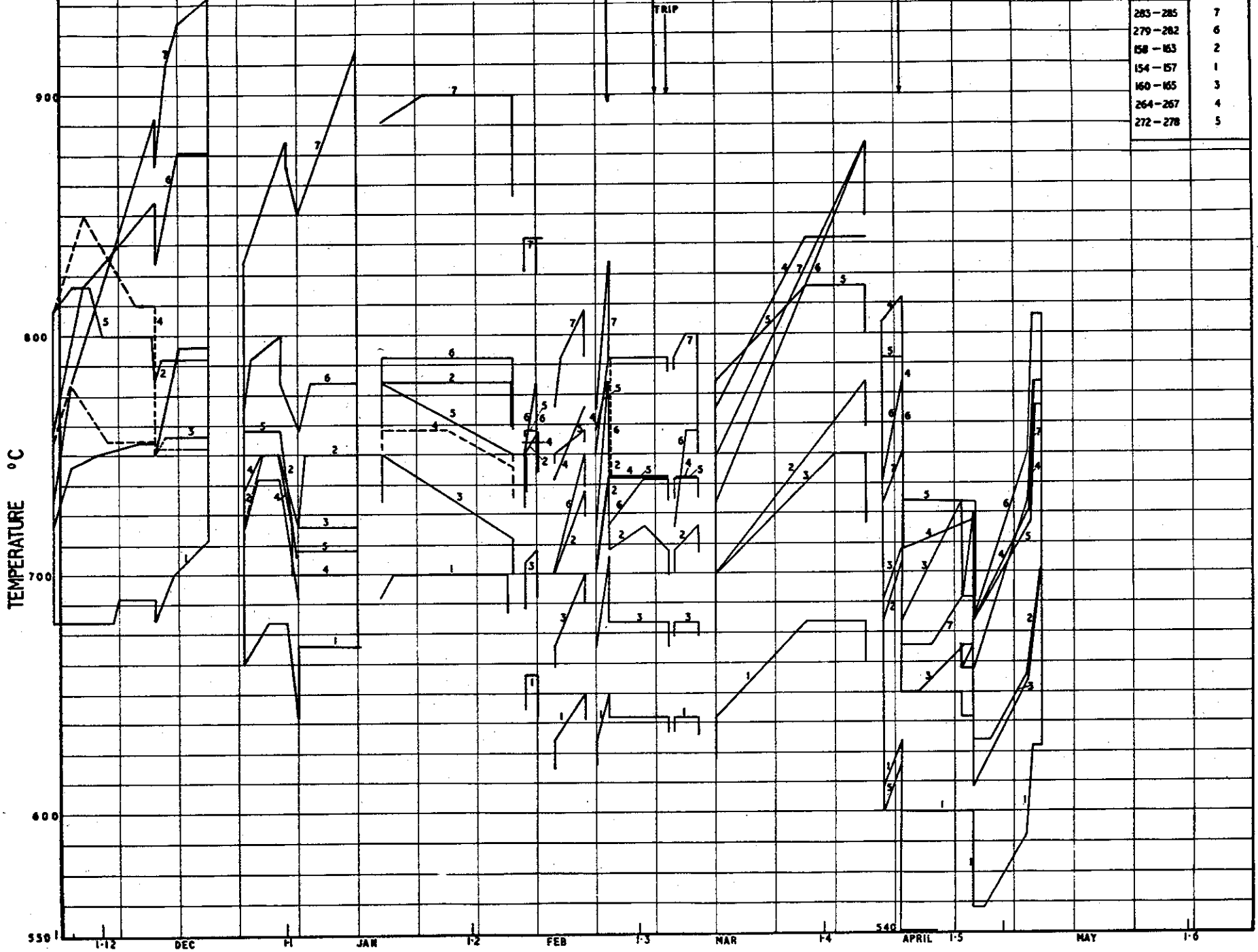

FIGURE 1 TEMPERATURE HISTORY CHART OF SPECIMENS IN STRINGER B

P 579

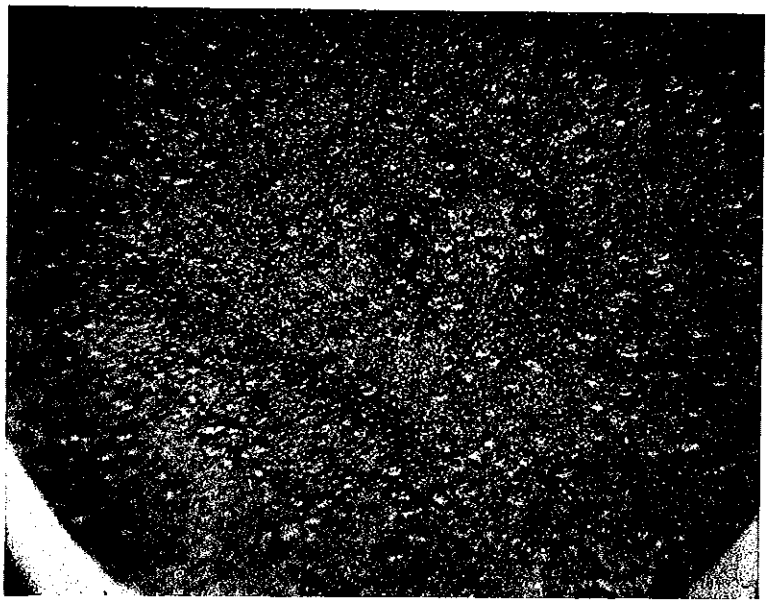

x 13

(a) Specimen 161
(2.6 a/o (U + Th) burn-up)

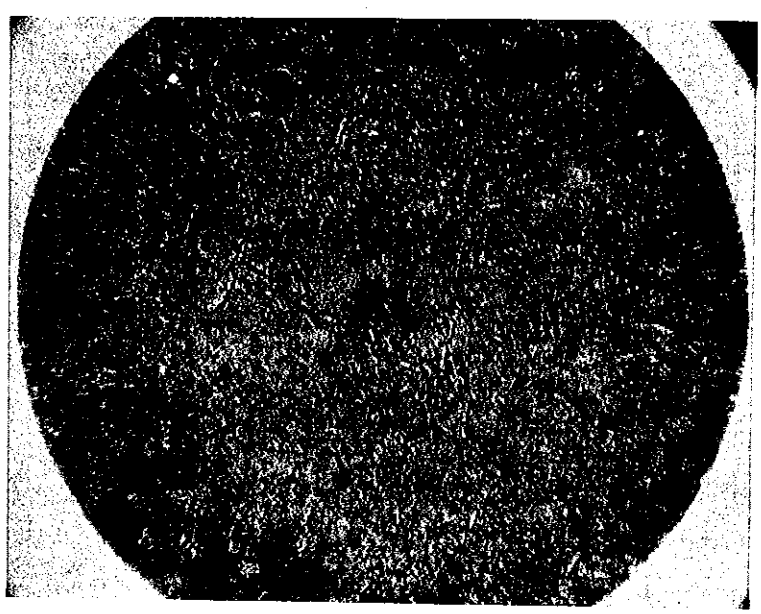

x 13

(b) Specimen 273
(5.5 a/o (U + Th) burn-up)

FIGURE 2 PHOTOGRAPHS OF THE END FACES OF IRRADIATED SPECIMENS

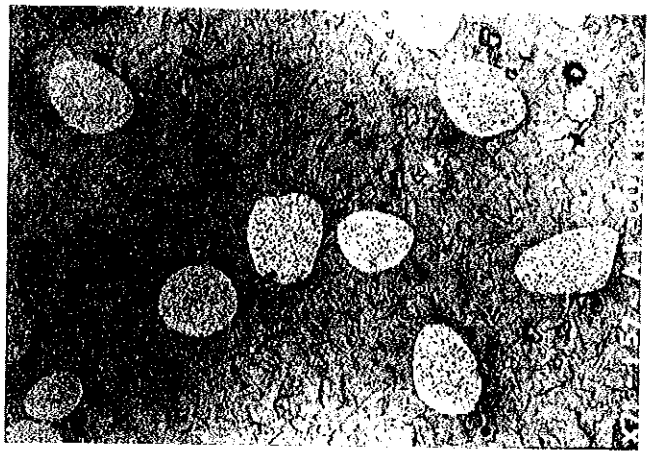

(a) unirradiated x 50

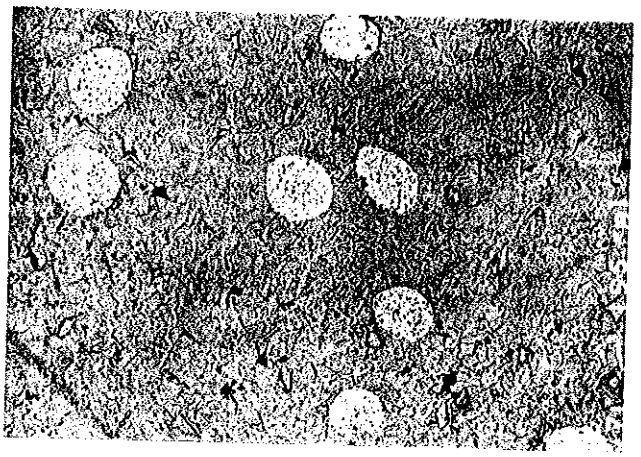

(b) 2.6 a/o burn-up of U +Th x 50

FIGURE 3 MICROSTRUCTURES OF SPECIMEN 155

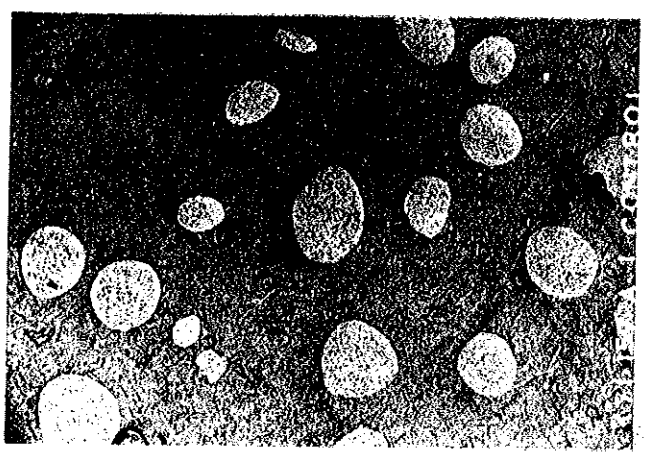

(a) unirradiated x 50

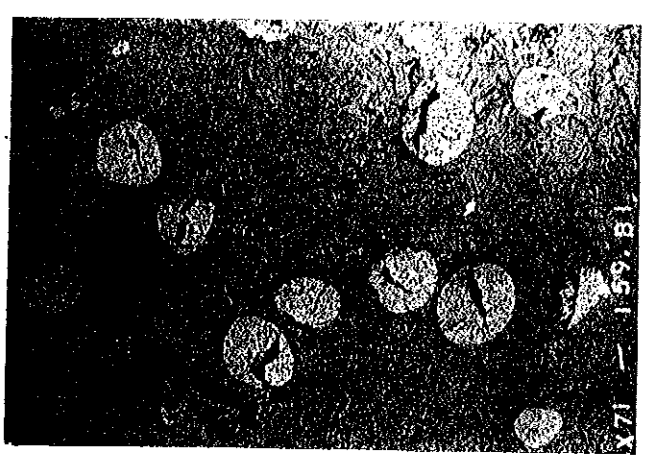

(b) Specimen 159
(2.5 a/o burn-up of U +Th) x 50

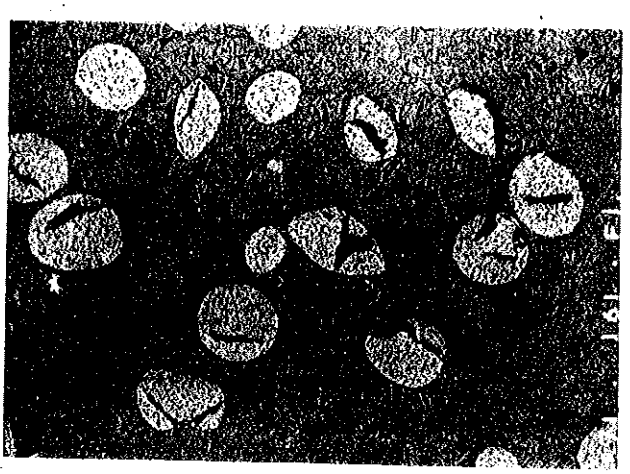

(c) Specimen 161
(2.6 a/o burn-up of U +Th) x 50

FIGURE 4 MICROSTRUCTURES OF SPECIMENS 159 AND 161

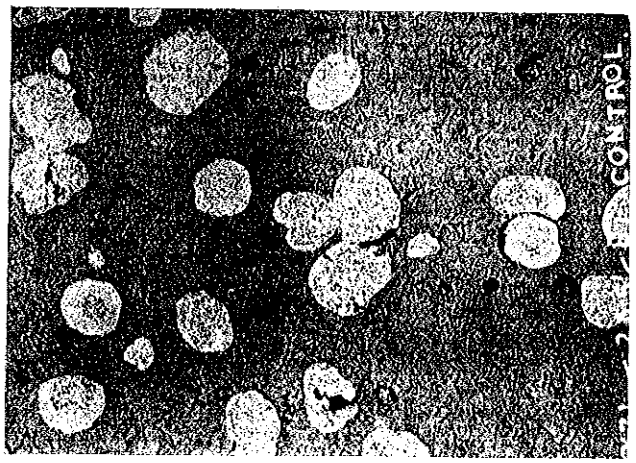

x 50

(a) unirradiated

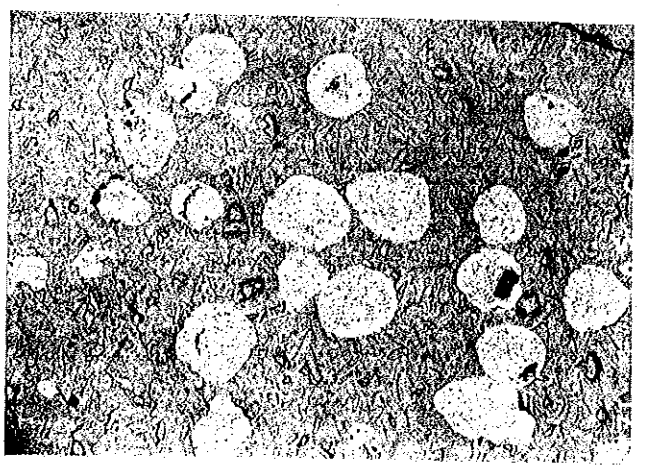

x 50

(b) 3.9 a/o burn-up of U + Th

FIGURE 5 MICROSTRUCTURES OF SPECIMEN 265

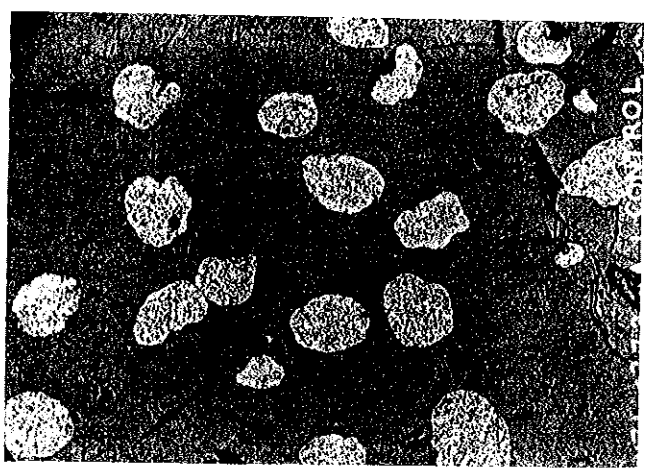

x50

(a) unirradiated

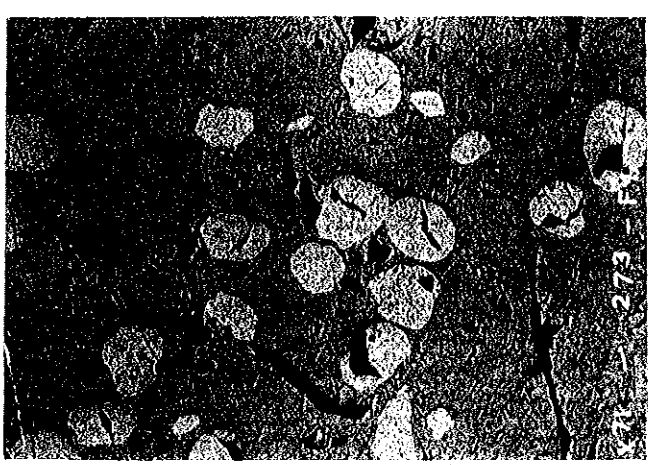

x 50

(b) 5.5 a/o burn-up of U + Th

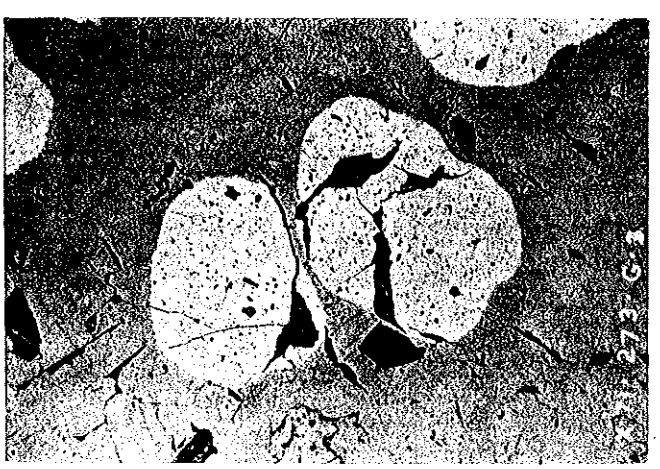

x 160

(c) 5.5 a/o burn-up of U + Th

FIGURE 6 MICROSTRUCTURES OF SPECIMEN 273

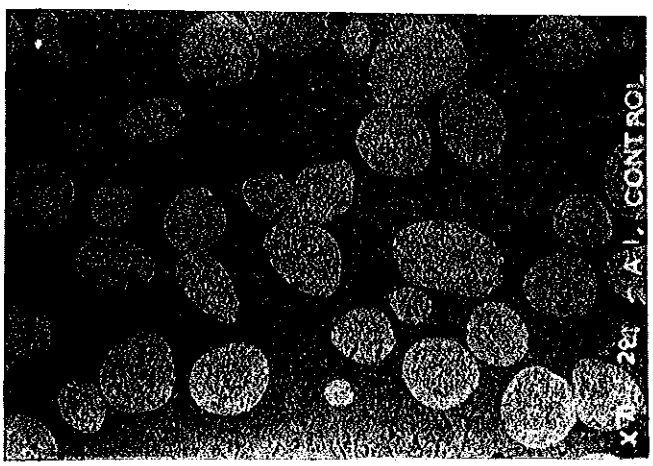

(a) unirradiated x 50

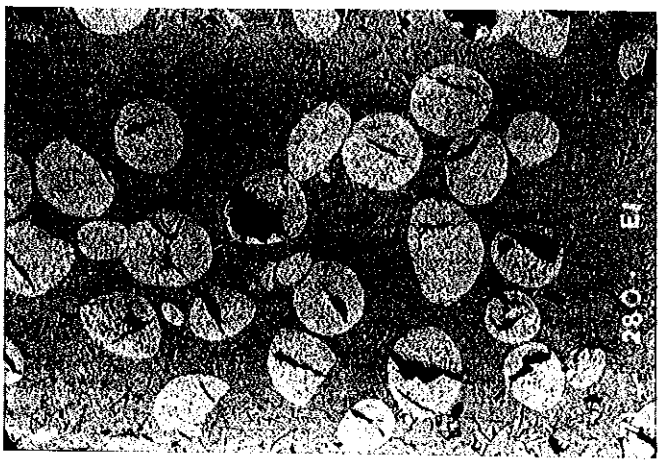

(b) 1.9 a/o burn-up of U +Th x 50

FIGURE 7 MICROSTRUCTURES OF SPECIMEN 280

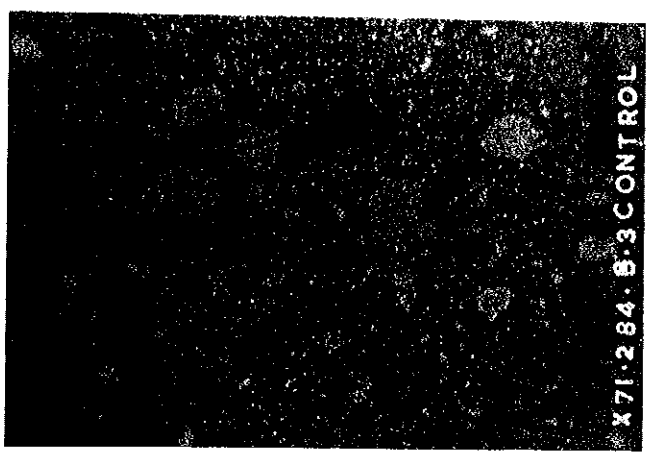

(a) unirradiated x 160

(b) 5.0 a/o burn-up of U +Th x 160

FIGURE 8 MICROSTRUCTURE OF SPECIMEN 284

(a) Specimen 161 (2.6 a/o burn-up of U +Th) x 525

(b) Specimen 273 (5.5 a/o burn-up of U +Th) x 525

FIGURE 9 FUEL-MATRIX INTERFACES IN IRRADIATED SPECIMENS

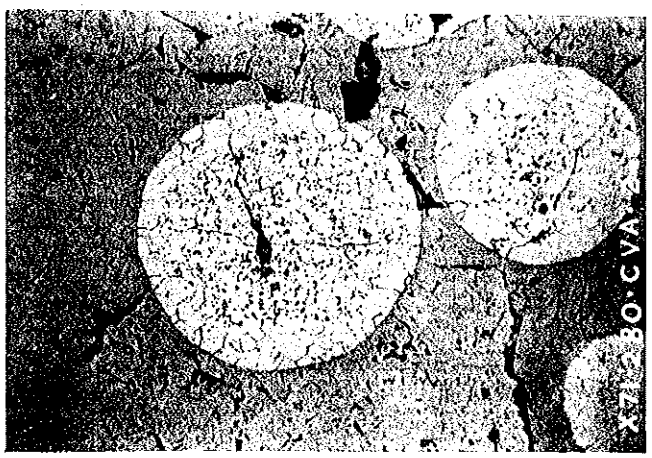

(a) Specimen 280 x 160
(1.9 a/o burn-up of U + Th)

(b) Specimen 273 x 160
(5.5 a/o burn-up of U + Th)

FIGURE 10 MICROSTRUCTURES OF SPECIMENS ANNEALED AT 1250 °C AFTER IRRADIATION

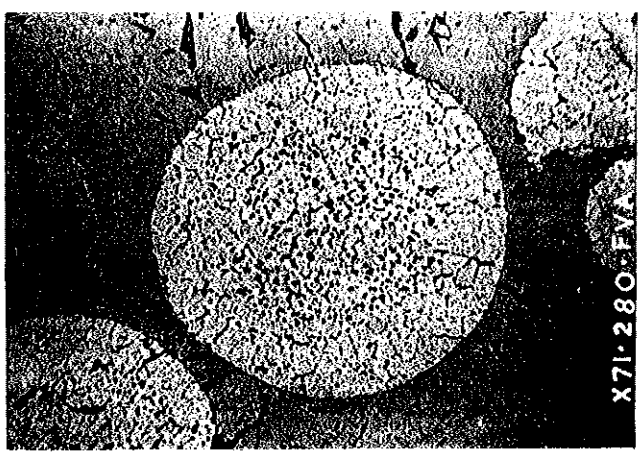

(a) Specimen 280 x 160
(1.9 a/o burn-up of U + Th)

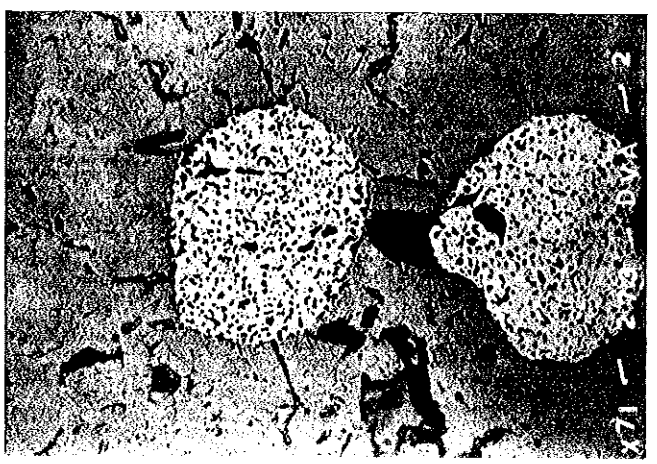

(b) Specimen 273 x 160
(5.5 a/o burn-up of U + Th)

FIGURE 11 MICROSTRUCTURES OF SPECIMENS ANNEALED AT 1500 °C AFTER IRRADIATION

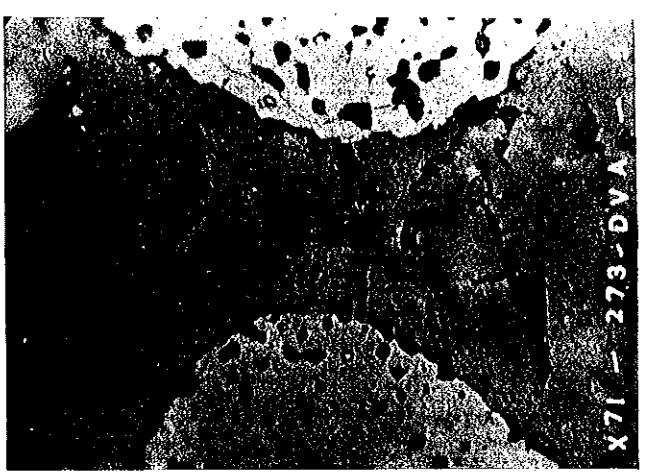

x 525

FIGURE 12 MICROSTRUCTURE OF FUEL–BeO INTERFACE IN SPECIMEN 273 AFTER ANNEALING AT 1500 °C

(Compare with Figure 9b)